This paper is available on line at http://www.mcponline.org

Wnt3a-dependent and -independent Protein Interaction Networks of Chromatin-bound β-catenin in Mouse Embryonic Stem Cells

Toma Yakulov§, Angelo Raggioli§, Henriette Franz‡, and Rolf Kemler§¶

Canonical Wnt signaling is repeatedly used during development to control cell fate, and it is often implicated in human cancer. β-catenin, the effector of Wnt signaling, has a dual function in the cell and is involved in both cell adhesion and transcription. Nuclear β-catenin controls transcription through association with transcription factors of the TCF family and the recruitment of epigenetic modifiers. In this study, we used a strategy combining the genetic manipulation of mouse embryonic stem cells with affinity purification and quantitative mass spectroscopy utilizing stable isotope labeling with amino acids in cell culture to study the interactome of chromatin-bound β-catenin with and without Wnt3a stimulation. We uncovered previously unknown interactions of β-catenin with transcription factors and chromatin-modifying complexes. Our proof-of-principle experiments show that β-catenin can recruit the H3K4me2/1 demethylase LSD1 to regulate the expression of the tumor suppressor *Lefty1* in mouse embryonic stem cells. The mRNA levels of *LSD1* and *β-catenin* are inversely correlated with the levels of *Lefty1* in pancreas and breast tumors, implying that this mechanism is common to mouse embryonic stem cells and cancer cells. ***Molecular & Cellular Proteomics 12: 10.1074/mcp.M112.026915, 1980–1994, 2013.***

The canonical Wnt signaling pathway plays multiple roles in development and is often dysregulated in human cancers (1). The key event in the canonical Wnt signaling is the regulation of β-catenin. Under normal conditions, the levels of β-catenin are low as a result of its phosphorylation by the destruction complex and subsequent ubiquitination and degradation by the proteasome (1). The destruction complex contains the scaffold proteins APC and Axin1, protein phosphatase 2a, and the kinases glycogen synthase kinase (GSK)-3β and casein kinase I alpha. Upon binding of Wnt ligands to the receptors Frizzled and LRP5/6, the destruction complex is turned off via translocation to the plasma membrane, where it binds Dishevelled. Thus, β-catenin is stabilized, translocates to the nucleus, and associates with TCF factors and with various proteins that are implicated in chromatin structure and RNA polymerase II regulation (1, 2).

The interactions of β-catenin with chromatin effector proteins are concentrated at the C-terminal domain of β-catenin, as shown for the histone acetyltransferases CBP and p300, the histone methyltransferase MLL, the nucleosome repositioning SWI/SNF family member protein Brg1, the Mediator component MED12, and the BCL-9/Pygo complex, which has the ability to bind methylated H3K4 (2). It is not probable that all these bulky multiprotein assemblies simultaneously occupy the C-terminal domain of β-catenin. Other transcription factors use the same repertoire of co-activators via sequential or cycling recruitment (3). It is likely that β-catenin serves as a platform which orchestrates the sequential recruitment of chromatin remodeling factors in a stimulus-dependent manner.

In mES[1] cells, the epigenetic regulation of gene expression has been shown to take place at the levels of DNA methylation, histone modification, nucleosome packaging and rearrangement, and higher order chromatin organization (4). Unique to key developmental genes in mES cells are bivalent chromatin domains with both activating and repressing marks, which contribute to the pluripotency potential of mES cells (5). Although Wnt/β-catenin signaling has been shown to play a role in the self-renewal and pluripotency of mES cells (6), the nuclear interaction partners of β-catenin in mES cells have not been extensively studied. Because mES cells have low intrinsic Wnt signaling activity, which can be further stimulated by the addition of exogenous Wnt3a (7), they are an excellent model for studying the dynamics of β-catenin complex formation upon Wnt3a stimulation.

In this study we used affinity purification and mass spectroscopy combined with stable isotope labeling with amino acids in cell culture (SILAC) to identify the Wnt3a-dependent and -independent chromatin interactomes of β-catenin in mES. We show the dynamics of complex formation upon Wnt3a treatment and identify among the β-catenin interaction

From the §Department of Molecular Embryology, Max Planck Institute of Immunobiology and Epigenetics, 79108 Freiburg, Germany; ‡Urologische Klinik/Frauenklinik und Zentrale Klinische Forschung, Klinikum der Universitaet Freiburg, 79106 Freiburg, Germany

Received December 21, 2012, and in revised form, March 5, 2013
Published, MCP Papers in Press, April 15, 2013, DOI 10.1074/mcp.M112.026914

[1] The abbreviations used are: ChIP, chromatin immunoprecipitation; GO, Gene Ontology; mES, mouse embryonic stem (cells); SILAC, stable isotope labeling with amino acids in cell culture.

partners both repressing and activating chromatin effector proteins. We found that β-catenin can associate with the H3K4me1/2 histone demethylase LSD1 to repress transcription. LSD1 is recruited to the proximal enhancer of *Lefty1* in a β-catenin-dependent manner, and *Lefty1* is up-regulated in β-catenin$^{-/-}$ cells, which correlates with increased H3K4me2/3 levels at the *Lefty1* proximal enhancer element.

EXPERIMENTAL PROCEDURES

Cell Culture and Labeling—SR1-Cre-ERT2 cells were routinely cultured on feeder cells in mES cell medium (Dulbecco's modified Eagle's medium supplemented with 15% fetal calf serum, 1:1000 in-house produced LIF, 1 mM penicillin/streptomycin, 2 mM L-glutamine, 1 mM sodium pyruvate, 1x non-essential amino acids, and 0.1 mM 2-mercaptoethanol) at 37 °C in a humidified atmosphere and 8% CO_2. For labeling, the cells were cultured in ES cell medium on gelatinized plates without feeders. One cell population was supplemented with normal isotope containing L-lysine and L-arginine (Sigma-Aldrich Corporation, St. Louis, MO), and another with heavy isotope labeled $^{13}C_8$-lysine and $^{13}C_6{}^{15}N_4$-arginine (Sigma-Aldrich Corporation, St. Louis, MO), generating mass shifts of +8 and +10 Da, respectively. mES cells were grown for 6 days in labeling medium before further treatment.

Cell Treatment—Wnt3a (R&D Systems, Minneapolis, MN) was used at a concentration of 150 ng/ml. The GSK3 inhibitor SB-216763 (Sigma-Aldrich Corporation, St. Louis, MO) was used at a concentration of 10 μM. LiCl was used at a concentration of 40 mM. (Z)-4-hydroxytamoxifen (Sigma-Aldrich Corporation, St. Louis, MO) was used at a concentration of 100 ng/ml. (Z)-4-hydroxytamoxifen was added to the medium on day 1, and 24 h later the cell medium was replaced with medium without (Z)-4-hydroxytamoxifen. 72 h after treatment, the cells were harvested.

Protein Extract Preparation—The cells were harvested by being scraped off the plates in Dulbecco's PBS without Ca and Mg (PAA Laboratories, Pasching, Austria) and lysed in Buffer A (1 mM Hepes pH 7.6, 0.5% Nonidet P-40, 0.5 mM $MgCl_2$, 1 mM DTT with protease inhibitors (EDTA-free protease inhibitor mixture, Roche, Mannheim, Germany), and phosphatase inhibitors (50 mM sodium fluoride, 1 mM sodium orthovanadate)). The cells were incubated for 20 min at 4 °C and then vortexed for 30 s. The chromatin was collected via 10 min of centrifugation at 2500 × *g*, and the supernatant was transferred to a new tube (soluble fraction). The buffer was adjusted to 10 mM Hepes pH 7.6, 100 mM NaCl, 1 mM $MgCl_2$. The chromatin fraction was washed twice with Buffer B (10 mM Hepes pH 7.6, 1 mM $MgCl_2$, 100 mM NaCl, 1 mM DTT with protease inhibitors (EDTA-free protease inhibitor mixture, Roche, Mannheim, Germany), and phosphatase inhibitors (50 mM sodium fluoride, 1 mM sodium orthovanadate)), and the DNA and RNA were digested via incubation in Buffer B with 1 kU benzonase (Sigma-Aldrich Corporation, St. Louis, MO) for 15 min at 25 °C (the chromatin-bound fraction). The soluble fraction and the chromatin-bound fraction were centrifuged for 15 min at 20,000 × *g* to remove residual cell debris and membranes.

Co-immunoprecipitation—The protein concentration of each extract was determined via Bradford assay (Thermo Fisher Scientific, Rochester, NY). For each reaction, 1.5 mg of total protein extract and 5 μg of anti-β-catenin antibody (Cell Signaling Technology, Danvers, MA) were used. The protein extract was incubated with the antibody for 2 h at 4 °C with rotation. The antibody-bound material was collected via the addition of 30 μl pre-washed magnetic Dynabeads ProteinG (Invitrogen, Carlsbad, CA). The beads were washed three times with 1 ml of Buffer B. Beads from parallel co-immunoprecipitations using light and heavy labeled extracts were mixed (8), and bound proteins were eluted in LDS sample buffer (Invitrogen, Carlsbad, CA).

Western Blotting—The primary antibodies used were anti-β-catenin produced in rabbit (1:1000, Cell Signaling Technology, Danvers, MA), anti-E-cadherin produced in mouse (1:1000, BD, Heidelberg, Germany), anti-Lamin B produced in goat (1:1000, Santa Cruz Biotechnology, Santa Cruz, CA), anti-OCT-3/4 produced in goat (1:1000, Santa Cruz Biotechnology, Santa Cruz, CA), anti-SOX2 produced in goat (1:1000, Santa Cruz Biotechnology, Santa Cruz, CA), anti-GAPDH produced in mouse (Merck, Darmstadt, Germany), anti-LSD1 produced in rabbit (Cell Signaling Technology, Danvers, MA), and anti-SALL4 produced in mouse (Merck, Darmstadt, Germany). The secondary antibodies were peroxidase conjugated anti-rabbit IgG and anti-mouse IgG produced in goat and anti-goat IgG produced in rabbit (Jackson Immunoresearch Laboratories, West Grove, PA).

LC-MS/MS—The fractionated cell extracts or the eluted proteins from the co-immunoprecipitations were separated on 4%–12% gradient SDS-PAGE gels (Invitrogen, Carlsbad, CA) and stained with colloidal Coomassie Blue. Each gel lane was cut into 12 equal gel slices, and the proteins from each gel slice were in-gel digested with trypsin (Promega, Madison, WI) as described elsewhere (9). Tryptic peptides from each gel slice were analyzed via nanoflow HPLC (Agilent, Boeblingen, Germany) coupled to a nanoelectrospray LTQ-Orbitrap XL mass spectrometer (Thermo Fisher Scientific, Waltham, MA) operating in positive ion mode. Peptides were desalted and subsequently separated on an analytical column (15 cm length and 75 μm inner diameter, packed into a picotip emitter with an 8 μm tip opening) at flow rate of 250 nl/min and a linear gradient of 2%–60% buffer B (80% acetonitrile and 0.5% acetic acid) for 50 min. Data-dependent acquisition of eluting peptides was applied and consisted of one survey scan in the Orbitrap with the resolution set at 60,000 at *m/z* 400 and the automatic gain control target at 10^6, followed by MS/MS of the five most intense precursors in the LTQ using collision-induced decay fragmentation with previously fragmented ions dynamically excluded for 90 s. The general mass spectrometric conditions were as follows: spray voltage, 2.3 kV; no sheath and auxiliary gas flow; ion transfer tube temperature, 160 °C; collision gas pressure, 1.3 mTorr; normalized collision energy using wide-band activation mode; 35% for MS^2. Ion selection thresholds were 500 or 1000 counts for MS^2, depending on the experiment. An activation q = 0.25 and activation time of 30 ms were applied.

Data Analysis—The raw files from the LTQ-Orbitrap XL were analyzed using MaxQuant software (version 1.0.13.13) (10). Peak lists generated by the first module of MaxQuant (Quant.exe) were queried by the Mascot search engine (Mascot Daemon 2.2, Matrix Science, London, UK) against the mouse International Protein Index database (version 3.87) supplemented with a list of frequent contaminants and concatenated with the reverse sequences of all entries. The total number of sequences in the database was 110,425. Enzyme specificity was set to trypsin with up to three missed cleavages and allowing cleavages N-terminal to proline and C-terminal to aspartate. Modifications were cysteine carbamidomethylation (fixed), protein N-terminal acetylation, asparagine and glutamine deamidation, and methionine oxidation (variable). The maximum mass deviations for monoisotopic precursor ions and MS/MS peaks were restricted to 5 ppm and 0.5 Da, respectively. The peptides were filtered for a maximum false discovery rate of 1% in MaxQuant. Only unique and razor peptides with a posterior error probability of less than 0.05 and proteins with a ratio count of at least three were accepted and used for quantification (10). All proteins are listed in supplemental Tables S1–S4 with accession numbers, numbers of unique peptides, percent sequence coverage, quantification significance, and variability as recorded by MaxQuant.

Gene Ontology Analysis—Gene Ontology (GO) term enrichment analysis was performed with AmiGO version 1.8 (11) using the GO database (released September 29, 2012). The database filter was set to MGI, and the default settings were used. The enriched GO terms were plotted with REViGO (12) with the "allowed similarity" set to large.

Proximity Ligation Assay—The DuoLink assay by Olink Bioscience (Uppsala, Sweden) was used according to the manufacturer's instructions. The primary antibodies used were anti-β-catenin produced in rabbit (1:100, Cell Signaling Technology, Danvers, MA), anti-β-catenin produced in mouse (1:100, BD Biosciences, Heidelberg, Germany), anti-SALL4 produced in mouse (1:100, Merck, Darmstadt, Germany), anti-LSD1 produced in rabbit (1:100, Cell Signaling Technology, Danvers, MA), and anti-HMG2 produced in rabbit (1:100, Sigma-Aldrich Corporation, St. Louis, MO).

Graphical Representation of Proteomics Data—For the graphical representation, R version 2.14.1 (13) was used. The scripts are available in the supplemental "Experimental Procedures" section.

Chromatin Immunoprecipitation—For ChIP, five confluent 15 cm dishes were used per experiment. The cells were fixed with 1% formaldehyde for 15 min at room temperature. After three washes with PBS, the cells were harvested with silicon scrapers and put on ice. Cells were lysed in lysis buffer (50 mM Tris pH 8.1, 150 mM NaCl, 10 mM EDTA, 1% SDS) and sonicated to shear the crosslinked DNA. For sonication we used the Covaris S2 system using the following parameters: 12 cycles, 15% duty cycle, intensity = 10, 500 cycle burst, 60 s duration, and frequency sweeping mode. 5 μg of each antibody were incubated overnight with cell extract containing 250 μg of DNA. Subsequently, Dynal Protein G magnetic beads were added for 1 h. The beads were washed four times for 4 min with low-salt buffer (20 mM Tris pH 8.1, 150 mM NaCl, 2 mM EDTA, 1% Triton X-100, 0.1% SDS) and once with high-salt buffer (20 mM Tris pH 8.1, 500 mM NaCl, 2 mM EDTA, 1% Triton X-100, 0.1% SDS). The immune complexes were eluted in 100 μl of elution buffer (1% SDS, 100 mM $NaHCO_3$) with RNase A and protease K to 500 μg/ml at 37 °C for 1 h. Crosslinking was reversed by overnight incubation at 65 °C. Whole cell extract DNA (reserved from the sonication step) was also subjected to crosslink reversal. The following antibodies were used: anti-LSD1 raised in rabbit (Abcam, Cambridge, UK), anti-β-catenin raised in mouse (1:5, in-house produced), anti-H3K4me2/3 raised in mouse (Abcam, Cambridge, UK), rabbit-IgG (Diagenode, Liège, Belgium), mouse-IgG (Santa Cruz Biotechnology, Santa Cruz, CA), and rabbit-IgG (Santa Cruz Biotechnology, Santa Cruz, CA). The qPCR analysis was performed as described elsewhere (14). The primers encompassing the *Lefty1* enhancer have been described elsewhere (14) and are 5′-GTAGCCAGCAGACAGGACAA-3′ and 5′-ATCCCCAATCCACATTCACT-3′. All data were first normalized to the percentage of input, including the IgG control. Because the IgG control represents the noise, the noise/input was subtracted from the signal/input. The average of two biological experiments was plotted with error bars showing the standard error of the mean.

Real-time PCR—Total RNA was isolated using an RNeasy Mini Kit (Qiagen, Hilden, Germany). cDNA was prepared using a RevertAid First Strand cDNA Synthesis Kit (Thermo Fisher Scientific, Rochester, NY). qPCR was performed using Absolute SYBR Green ROX mix (Thermo Fisher Scientific, Rochester, NY). The primer sequences for *Lefty1* were 5′-ACTCAGTATGTGGCCCTGCTA-3′ and 5′- AACCTGCCTGCCACCTCT-3′. The primer sequences for *Tbp* were 5′-CGGTCGCGTCATTTTCTC-3′ and 5′-GGGTTATCTTCACACACCATGA-3′. The results represent the average of three experiments performed in triplicate, and the error bars show the standard error from the mean.

In Silico Binding Protein Analysis—Known and predicted protein associations were analyzed and visualized with STRING version 9.0 (15). The Active Prediction Methods used were "Experiments," "Databases," and "Textmining," with "Required Confidence" set to "low confidence (0.150)."

Statistical Analysis—The statistical analysis was done in Excel. The *p* values for the data represented in Fig. 6 were determined via one-tailed Student's *t* test. Pearson correlation was done in Excel. In the pancreas cancer dataset (PubMed ID 19260470), the relative fold change between the tumor and the normal tissue was used. In premalignant breast cancer samples, the measured values were taken.

RESULTS

Experimental Setup—In order to study the interactome of β-catenin via co-immunoprecipitation from metabolically labeled cells using SILAC, we needed a cell system in which we could identify the β-catenin binding proteins before large changes in the proteome had taken place. For that, we took advantage of the SR1-Cre-ERT2 system.[2] It has been previously shown that β-catenin$^{flox/-}$ mES cells are phenotypically wild type (16). SR1-Cre-ERT2 cells are β-catenin$^{flox/-}$ cells that have been stably transfected with a vector carrying tamoxifen-inducible Cre recombinase. The addition of tamoxifen to the medium causes the removal of the β-catenin sequence between the two *loxP* sites via recombination, thereby generating β-catenin$^{-/-}$ mES cells (Fig. 1*A*) (17). Three days after the induction of recombination, β-catenin was not detectable via Western blot (Fig. 1*B*).

In order to study the interactome of chromatin-bound β-catenin, we set out to establish a protocol that would allow us to separate the chromatin-bound from the soluble β-catenin. As a criterion for successful separation, we used a Western blot for E-cadherin, which binds β-catenin at the cell membrane (18). The separation of the cytoplasmic and the nuclear β-catenin with commercially available kits was not appropriate, because we could detect E-cadherin in the nuclear fraction (Fig. 1*C*). To solve this problem, we developed a one-step protocol wherein the Nonidet P-40 detergent concentration was essential. After fractionation, E-cadherin was detected in the soluble, but not in the chromatin, fraction (Fig. 1*D*). The transcription factors OCT-3/4 and SOX2 were found exclusively in the chromatin fraction (19–21), along with Lamin B, a major component of the nuclear lamina (22) (Fig. 1*D*). Thus, our fractionation procedure could successfully separate the chromatin-bound β-catenin from the soluble β-catenin.

To prepare the labeled protein extracts, we grew SR1-Cre-ERT2 cells under SILAC conditions. We used medium containing normal isotope L-arginine and L-lysine for preparing the "light" extracts and medium containing heavy isotope labeled $^{13}C_6{}^{15}N_2$-lysine (Lys+8) and $^{13}C_6{}^{15}N_4$-arginine (Arg+10) for preparing the "heavy" extracts. Both the soluble and the chromatin fractions from the tamoxifen- and mock-treated cells were tested to ensure the high similarity of the heavy and light material (*i.e.* the extracts contained mostly the same proteins in the same amounts, as judged by their ratios).

[2] Raggioli *et al.*, in preparation.

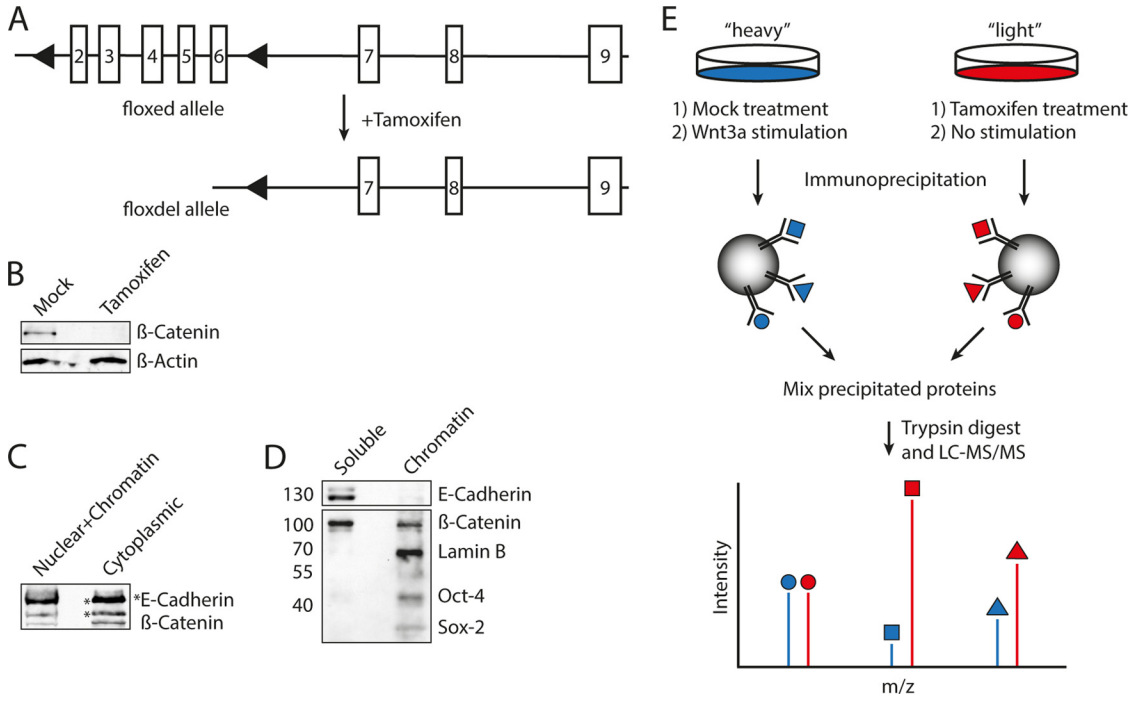

FIG. 1. **Experimental setup for the affinity purification of chromatin-bound β-catenin interacting partners.** *A*, scheme of the β-catenin^{flox} allele. Upon treatment with tamoxifen, the genomic sequence from exon two to exon six is recombined to delete the remaining β-catenin. *B*, Western blot of total cell extracts from SR1-Cre-ERT2 after 3 days of mock or tamoxifen treatment. Treatment of these cells with tamoxifen leads to a loss of β-catenin. *C*, *D*, optimization of the biochemical procedure for the separation of the chromatin-bound β-catenin from the cytoplasmic β-catenin. *C*, Western blot with anti-E-cadherin and anti-β-catenin antibodies after a standard fractionation shows that the nuclear/chromatin fraction was still contaminated with membrane proteins. *D*, Western blot with antibodies against membrane (E-cadherin) and chromatin (OCT4, SOX2, LaminB) proteins. An optimized protocol yields a clear separation between the membrane/cytoplasmic and chromatin fractions of β-catenin. *E*, schematic representation of the affinity purification and of the protein identification procedures.

In the forward experiments, the mock-treated cells were incubated with the heavy medium and the tamoxifen-treated cells were incubated with the light medium. In the reverse experiments, the labeling was swapped. The extracts were analyzed at 3 days after the induction of recombination (supplemental Figs. S1*A* and S1*B*, supplemental Tables S1 and S2). As expected, β-catenin was efficiently down-regulated, as judged by the heavy-to-light normalized ratios of 4.9 in the chromatin fraction (supplemental Table S1) and 12.6 in the soluble fraction (supplemental Table S2). In the soluble fraction we identified 3643 proteins, of which 3533 proteins showed quantitative ratios (supplemental Table S2). Accordingly, from 2089 identified proteins in the chromatin fraction, we obtained quantitative ratios for 2026 proteins (supplemental Table S1). In both fractions, the quantitative ratios were grouped around 1:1, showing similar proteomes for the *β-catenin*$^{flox/-}$ and *β-catenin*$^{-/-}$ cells (supplemental Figs. S1*A* and S1*B*).

Wnt3a-independent Interactome of β-catenin in the Chromatin of mES Cells—To study the interactome of β-catenin in mES cells, we prepared chromatin extracts from SILAC labeled SR1-Cre-ERT2 cells that had been either mock- or tamoxifen-treated for 3 days. Two biological replicas, a forward and a reverse experiment, were performed. Equal amounts of heavy or light protein extracts were incubated with anti-β-catenin antibodies immobilized on magnetic beads (Fig. 1*E*). The beads were mixed before the last wash. The proteins that were retained by the antibodies were recovered and run on SDS-PAGE gels, and the separated proteins were trypsinized. The tryptic peptides were analyzed via electrospray ionization mass spectroscopy, and a heavy-to-light ratio for each SILAC pair was determined (Fig. 1*E*).

We identified 1034 proteins in the two biological replicas, of which 962 had quantitative ratios (Fig. 2*A*) (supplemental Table S3). β-catenin was specifically enriched in both forward and reverse experiments, with normalized ratios of 8.8 and 4.6, respectively (supplemental Table S3). To determine an empirical threshold for the specific enrichment of interaction partners in our experiment, we searched the list of identified SILAC pairs for known β-catenin interacting proteins. We found Pontin (RUVBL1) and Reptin (RUVBL2), two helicases that have been previously identified as nuclear β-catenin interaction partners (23, 24). They were enriched in both experiments, with normalized ratios of 2.0 and 1.6 for Pontin and 1.9 and 2.0 for Reptin in the forward and the reverse experiment, respectively (supplemental Table S3). Thus, we set as an enrichment threshold a normalized ratio of more than 1.5-fold in both the forward and the reverse experiments.

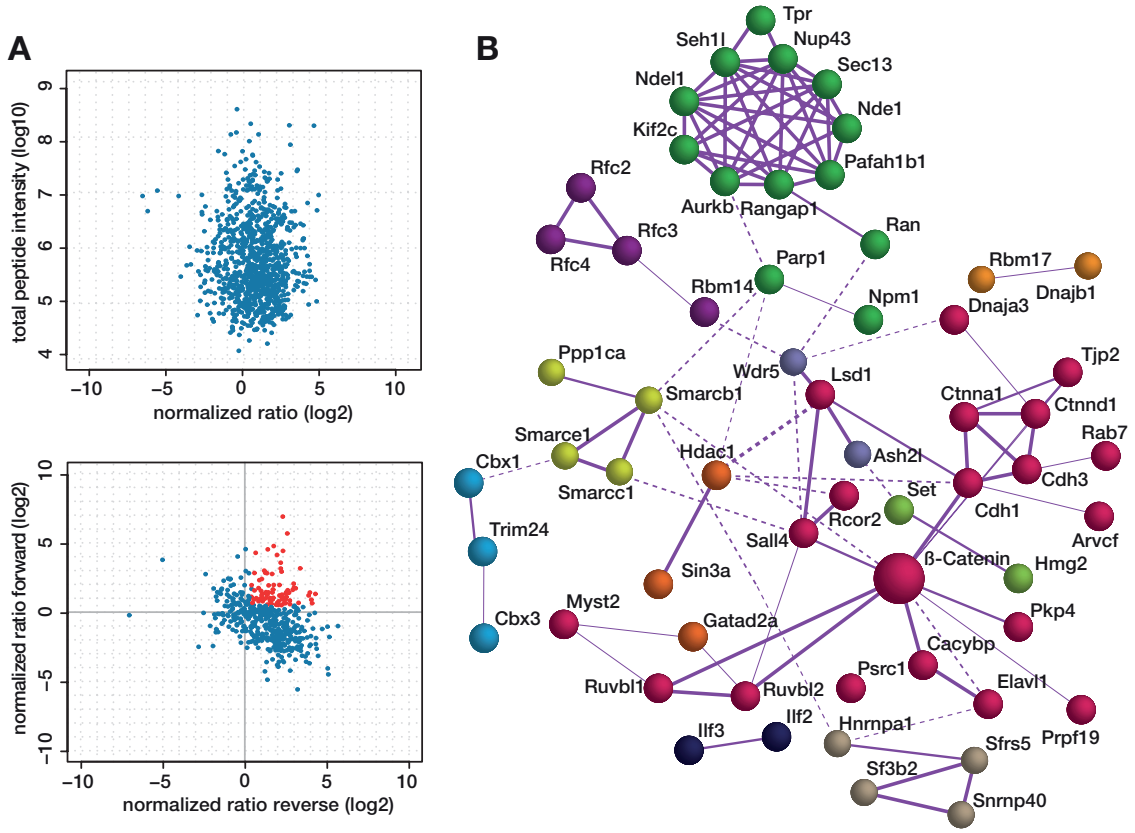

FIG. 2. **Wnt-independent interactome of the chromatin-bound β-catenin in mES cells.** *A* (upper panels), scatter plot of normalized heavy-to-light ratios of identified proteins and total peptide intensities. Proteins with quantitative ratios in both the forward and the reverse experiment, or in either of them, are represented on the graph. *A* (lower panels), scatter plot of normalized ratios of proteins with quantitative ratios in both forward and reverse experiments. Proteins with fold change ratios above 1.5 in both experiments are colored red. *B*, β-catenin interacting proteins of the Wnt-independent proteome with fold change ratios above 1.5 in the forward and reverse experiments were analyzed using the STRING protein interaction database (15). Only the proteins with known and predicted interactions are shown in the schematic drawing. The color code represents k-means clustering of the interaction likelihood among the different proteins. The thicker non-dashed lines between proteins represent high-confidence interactions, whereas thinner dashed lines between proteins represent low-confidence interactions.

When these criteria were applied to our dataset, 76 proteins were found to bind β-catenin specifically in the chromatin of mES cells (Wnt3a-independent interactome) (Table I). 20% of these proteins (16 of 76) have been previously shown to associate directly or indirectly with β-catenin (Table I). Thus, 80% of the Wnt3a-independent interactome comprises novel interaction partners of chromatin-bound β-catenin. A STRING (15) analysis of the Wnt3a-independent β-catenin interactome revealed a complex network of known or predicted functional interactions among the enriched proteins (Fig. 2*B*).

Wnt3a-dependent β-catenin Interactome in the Chromatin of mES Cells—In order to be able to directly compare the interactomes of β-catenin before and after Wnt3a treatment, we decided to study the same SR1-Cre-ERT2 cell line after Wnt3a stimulation. β-catenin$^{flox/-}$ cells respond to Wnt3a stimulation with the up-regulation of the canonical Wnt signaling targets *Axin2*, *Cdx1*, and *brachyury* (*T*) within 4 h after Wnt3a supplementation (25), and SR1-Cre-ERT2 are similarly Wnt3a responsive.[2] Interestingly, we could not observe a significant increase in the protein levels of chromatin-bound β-catenin in mES cells after Wnt3a, LiCl, or GSK3a inhibitor treatments (supplemental Fig. S2*A*). To study the interactome of β-catenin in mES cells after Wnt3a stimulation, we immunoprecipitated β-catenin from the chromatin of SILAC labeled SR1-Cre-ERT2 cells that had been mock or Wnt3a treated for 4 h. In the two biological replicas, the forward and the reverse experiments, we identified 1132 proteins in total, of which 1043 had quantitative ratios (Fig. 3*A*) (supplemental Table S4). The normalized ratios for β-catenin were 1.0 and 1.3, respectively. As a cutoff for enrichment, we used, as before, a normalized ratio of 1.5 in both the forward and the reverse experiments. We identified 69 proteins that matched our criteria (Wnt-3a-dependent interactome) (Fig. 3*B*) (Table II). Only 10% of those had been previously shown to associate with β-catenin (Table II), whereas 90% represented novel interaction partners. Interesting is the comparison of the β-catenin Wnt3a-independent and Wnt3a-dependent interactomes. 64 proteins of the Wnt3a-dependent interactome were found

TABLE I
Wnt3a-independent interactome of β-catenin

IPI number and gene name	Functional relevance[a]	Pfam descriptions
IPI00108271: Elavl1[b,c,d]	RNA binding	RNA recognition motif
IPI00111560: Set[d]	Nucleosome assembly	Nucleosome assembly protein
IPI00112460: Nde1[d]	Microtubule cytoskeleton organization	NUDE protein, C-terminal conserved region
IPI00112963: Ctnna1[b,d]	Cell adhesion	Vinculin family
IPI00114232: Hdac1[b,d]	Transcription cofactor activity	Histone deacetylase domain
IPI00114560: Rab1A[c,d]	Small GTPase signal transduction	Ras family
IPI00114945: Sept2	GTPase activity	Septin
IPI00115650: Cacybp[b]	Proteolysis	CS domain; SGS domain
IPI00116825: Abcf2	Pyrophosphatase activity	ABC transporter
IPI00117932: Sin3a[d]	Transcription corepressor activity	Histone deacetylase (HDAC) interacting
IPI00623506: Ank3[b,d]	Cell communication	Death domain; ZU5 domain; Ankyrin repeat
IPI00119111: Cnn3[d]	Actin binding	Calponin family repeat
IPI00119892: Smarce1[d]	Chromatin organization	HMG (high mobility group) box
IPI00122549: Vdac1[c,d]	Ion channel activity	Eukaryotic porin
IPI00123281: Lrrc59[d]		Leucine rich repeat
IPI00123365: Kif2c[d]	Microtubule motor activity	Kinesin motor domain
IPI00123557: Ruvbl2[b,d]	Histone acetyltransferase complex	ATPase family
IPI00124744: Rfc2[d]	DNA clamp loader activity	ATPase family
IPI00125662: Smarcc1[d]	SWI/SNF chromatin remodeling complex	Myb-like DNA-binding domain; SWIRM
IPI00127415: Npm1[d]	Transcription factor binding; rRNA binding	Nucleoplasmin
IPI00127472: Arvcf[b,d]	Cell adhesion	Armadillo/beta-catenin-like repeat
IPI00129145: Smarcb1[d]	Chromatin remodeling	SNF5/SMARCB1/INI1
IPI00129466: Cbx1[d]	Chromatin organization	Chromo domain
IPI00129468: Cbx3[d]	Chromatin organization	Chromo domain
IPI00828741: Raly[d]	mRNA processing	RNA recognition motif
IPI00130185: Ppp1ca[d]	Protein phosphatase activity	Calcineurin-like phosphoesterase
IPI00130591: Ilf3[d]	Regulation of transcription	Double-stranded RNA binding motif
IPI00131130: Trim24[d]	Regulation of transcription	Bromo domain; PHD-finger; B-box zinc finger
IPI00131513: Ash2l[b,d]	Histone methyltransferase complex	SPRY domain
IPI00133920: Sec13[d]		WD domain, G-beta repeat
IPI00133985: Ruvbl1[b,d]	Histone acetyltransferase complex	ATPase family
IPI00134621: Ran[b,c,d]	Nucleocytoplasmic transport	Ras family
IPI00136253: Dnajb1	Protein folding	DnaJ domain
IPI00139168: Parp1[b,d]	Telomere maintenance	Poly(ADP-ribose) polymerase
IPI00139957: Wdr5[b,d]	Histone methyltransferase complex	WD domain, G-beta repeat
IPI00170394: Rbm17[d]	RNA splicing factor activity	G-patch domain; RNA recognition motif
IPI00172197: Anln[d]	Actin binding	PH domain
IPI00177202: Nup43[d]	Nuclear pore	WD domain, G-beta repeat
IPI00222760: Prpf19[d]	Ubiquitin ligase complex	Prp19/Pso4-like; U-box domain; WD domain
IPI00223415: Nars	Aminoacyl-tRNA ligase activity	tRNA synthetase class II
IPI00404579: Rab5c	Small GTPase mediated signal	Ras family
IPI00226581: Rcor2[d]	Transcription corepressor activity	ELM2 domain; DNA-binding domain
IPI00515403: Myst2[d]	Histone acetyltransferase complex	MOZ/SAS family; zinc finger, C2HC type
IPI00625995: Gatad2a[b,d]	NuRD complex	
IPI00230355: Gspt1	Translation release factor activity	Elongation factor Tu domain 2
IPI00266526: Cdh3[b,d]	Cell adhesion	Cadherin domain
IPI00269661: Hnrnpa3	Spliceosomal complex	RNA recognition motif
IPI00347634: Dnaja3	Small GTPase regulator activity	DnaJ domain
IPI00309207: Pafah1b1[d]	Microtubule cytoskeleton organization	LisH; WD domain, G-beta repeat
IPI00314709: Sfrs5[c,d]	RNA binding	RNA recognition motif
IPI00315517: Seh1l	Nuclear pore	WD domain, G-beta repeat
IPI00318238: Ndel1[d]	Microtubule cytoskeleton organization	NUDE protein, C-terminal conserved region
IPI00318550: Ilf2[d]	Transcription regulator activity	DZF
IPI00318626: Cdh1[b,d]	Cell adhesion	Cadherin domain
IPI00653266: Rfc4[d]	DNA clamp loader activity	ATPase family
IPI00320259: Psrc1[d]	Microtubule cytoskeleton organization	
IPI00323349: Tjp2[b,d]		PDZ domain
IPI00330763: Fam76b[d]		
IPI00349401: Sf3b2[d]	mRNA processing	PSP; SAP domain
IPI00387315: Aurkb[d]	Protein serine/threonine kinase activity	Protein kinase domain

TABLE I—*continued*

IPI number and gene name	Functional relevance[a]	Pfam descriptions
IPI00752108: Ctnnd1[b,d]	Regulation of transcription	Armadillo/beta-catenin-like repeat
IPI00404707: Rbm14[d]	Transcription coactivator activity	RNA recognition motif
IPI00408892: Rab7a[d]	Small GTPase signal transduction	Ras family
IPI00411164: Etl4[d]		
IPI00454142: Sept11	Septin complex	Septin
IPI00648295: LSD1[d]	Negative regulation of transcription	SWIRM domain
IPI00461621: Snrnp40[d]	mRNA processing	WD domain, G-beta repeat
IPI00462291: Hmg2[b,c,d]	DNA bending activity	HMG (high mobility group) box
IPI00467338: Rangap1[b,d]	Ran GTPase activator activity	RanGAP1 C-terminal domain
IPI00473693: Pkp4[d]	Cell adhesion	Armadillo/beta-catenin-like repeat
IPI00474157: Tomm40	Voltage-gated ion channel activity	Porin_3
IPI00828722: Sall4[d]	Regulation of transcription	Zinc finger, C2H2 type
IPI00553777: Hnrnpa1[c,d]	RNA splicing	RRM_1
IPI00553798: Ahnak[d]		CheC-like family; PDZ domain
IPI00665571: Rfc3[d]	DNA replication	Clamp-loader complex subunit E C-terminus
IPI00880644: Tpr[d]	Nuclear pore complex-associated protein	TPR/MLP1/MLP2-like protein

[a] According to Gene Ontology.

[b] Proteins previously shown to associate directly or indirectly with β-catenin according to literature search.

[c] Proteins that were found with ratios of more than 1.5 in the biological replicas in both the Wnt3a-independent and the Wnt3a-dependent proteomes.

[d] Proteins found to bind β-catenin with ratios of less than 1.5 after Wnt3a stimulation.

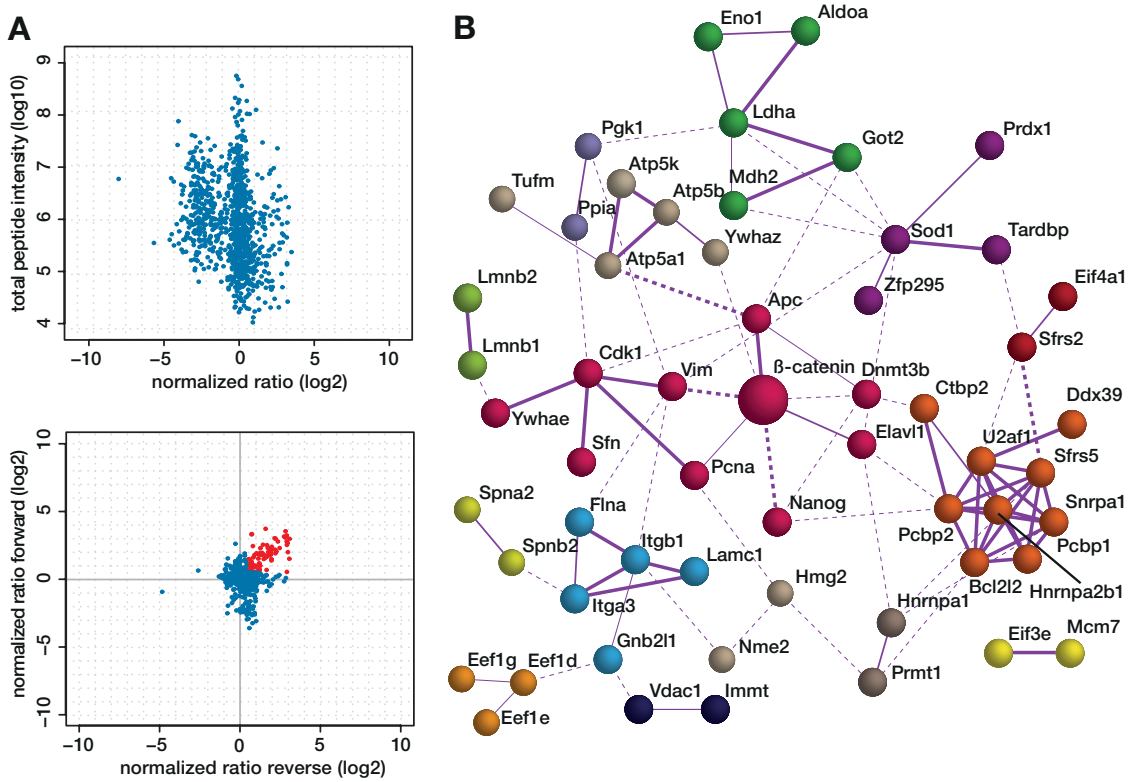

FIG. 3. **Wnt3a-dependent interactome of the chromatin-bound β-catenin in mES cells 4 h after Wnt3a stimulation.** *A* (upper panels), scatter plot of normalized heavy-to-light ratios of identified proteins and total peptide intensities. Proteins with quantitative ratios in both the forward and the reverse experiment, or in either of them, are represented on the graph. *A* (lower panels), scatter plot of normalized ratios of proteins with quantitative ratios in both the forward and the reverse experiment. Proteins with fold change ratios above 1.5 in both experiments are colored red. *B*, β-catenin interacting proteins of the Wnt-dependent proteome with fold change ratios above 1.5 in the forward and the reverse experiments were analyzed using the STRING protein interaction database (15). Only the proteins with known and predicted interactions are shown in the schematic drawing. The color code represents k-means clustering of the interaction likelihood among the different proteins. The thicker non-dashed lines between proteins represent high-confidence interactions, whereas thinner dashed lines between proteins represent low-confidence interactions.

TABLE II
Wnt3a-dependent interactome of β-catenin

IPI number and gene name	Functional relevance[a]	Pfam descriptions
IPI00117312: Got2	Transaminase activity	Aminotransferase class I and II
IPI00108125: Eif5a	Translation initiation factor activity	Eukaryotic initiation factor 5A hypusine
IPI00230394: Lmnb1	Structural molecule activity	Intermediate filament protein
IPI00126191: Lmnb2	Structural molecule activity	Intermediate filament protein
IPI00554989: Ppia	Peptidyl-prolyl cis-trans isomerase activity	Cyclophilin type peptidyl-prolyl cis-trans isomerase
IPI00462291: Hmg2[b,c]	DNA bending activity	HMG (high mobility group) box
IPI00318841: Eef1g	Translation elongation factor activity	Elongation factor 1 gamma
IPI00751369: Ldha	L-lactate dehydrogenase activity	Lactate/malate dehydrogenase
IPI00856379: Aldoa	Fructose-bisphosphate aldolase activity	Fructose-bisphosphate aldolase class-I
IPI00130589: Sod1	Superoxide dismutase activity	Cation transporting ATPase
IPI00944009: Eef1d	Translation elongation factor activity	Elongation factor 1 beta central acidic region
IPI00379441: Nme2	Nucleoside diphosphate kinase activity	Nucleoside diphosphate kinase
IPI00890117: Cfl1	Actin binding	Cofilin/tropomyosin-type actin-binding protein
IPI00378187: Rbm3	Ribosomal large subunit binding	RNA recognition motif
IPI00462072: Eno1	Carbohydrate metabolic process	Enolase
IPI00828488: Hnrnpa2b1	Single-stranded DNA binding; RNA binding	RNA recognition motif
IPI00308706: Rpl5	Structural constituent of ribosome	Ribosomal L18p/L5e family
IPI00118676: Eif4a1	Translation initiation factor activity	DEAD/DEAH box helicase
IPI00856974: Ctbp2[b]	Transcription corepressor activity	D-isomer specific 2-hydroxyacid dehydrogenase
IPI00277066: Hnrnpab	DNA replication origin binding	CBFNT (NUC161) domain; RNA recognition motif
IPI00553777: Hnrnpa1[c]	RNA splicing	RRM_1
IPI00227299: Vim	Intermediate filament	Intermediate filament protein
IPI00323592: Mdh2	Malate dehydrogenase activity	Lactate/malate dehydrogenase
IPI00122549: Vdac1[c]	Ion channel activity	Eukaryotic porin
IPI00230415: Eif2s3x	Translation initiation factor activity	Initiation factor eIF2 gamma, C terminal
IPI00119913: Apc[b]	Beta-catenin binding	APC 15 residue motif; APC basic domain
IPI00113870: Pcna[b]	DNA polymerase processivity factor activity	Proliferating cell nuclear antigen
IPI00123878: Ddx39	Helicase activity	DEAD/DEAH box helicase
IPI00121788: Prdx1	Peroxiredoxin activity	C-terminal domain of 1-Cys peroxiredoxin
IPI00626752: Bub3	Sister chromatid segregation	WD domain, G-beta repeat
IPI00108271: Elavl1[c]	RNA binding	RNA recognition motif
IPI00121758: Tardbp	DNA binding; RNA binding	RNA recognition motif
IPI00651876: Rab1a[c]	Intracellular signaling cascade	Ras family
IPI00127707: Pcbp2	DNA binding; RNA binding	KH domain
IPI00921658: Flna	Actin binding	Calponin homology (CH) domain
IPI00122547: Vdac2	Voltage-gated ion channel activity	Eukaryotic porin
IPI00468674: Itga3	Signal transducer activity	FG-GAP repeat; integrin alpha
IPI00331660: Tdh	Oxidoreductase activity	NAD dependent epimerase/dehydratase family
IPI00468481: Atp5b	Cation transmembrane transporter activity	ATP synthase alpha/beta family
IPI00555069: Pgk1	Phosphoglycerate kinase activity	Phosphoglycerate kinase
IPI00222496: Pdia6	Protein disulfide isomerase activity	Thioredoxin
IPI00118384: Ywhae	Intracellular protein transport	14-3-3 protein
IPI00318548: U2af1	RNA splicing	RNA recognition motif
IPI00132474: Itgb1	Signal transducer activity	EGF-like domain; integrin beta cytoplasmic domain
IPI00116498: Ywhaz[b]	Intracellular protein transport	14-3-3 protein
IPI00136169: Pabpn1	Poly(A) RNA binding	RNA recognition motif
IPI00319830: Sptbn1	Structural constituent of cytoskeleton	Calponin homology (CH) domain; PH domain
IPI00753815: Sptan1	Structural constituent of cytoskeleton	EF hand; SH3 domain; spectrin repeat
IPI00400016: Lamc1	Structural molecule activity	Laminin B (Domain IV); laminin EGF-like
IPI00128904: Pcbp1	Translation factor activity	KH domain
IPI00120495: Prmt1	Protein methyltransferase activity	
IPI00625588: Tufm	Translational elongation	Elongation factor Tu domains
IPI00114491: Cdc2[b]	Protein serine/threonine kinase activity	Protein kinase domain
IPI00132250: Eif3e	Translation factor activity	eIF3 subunit 6 N terminal domain; PCI domain
IPI00453824: Zfp295		BTB;zf-C2H2
IPI00117705: Ddost	Transferase activity	DDOST_48kD
IPI00929813: Nap1l1	Chromatin organization	Nucleosome assembly protein (NAP)
IPI00467338: Immt		Mitochondrial inner membrane protein
IPI00109731: Nanog	Transcription factor activity	Homeobox domain
IPI00111770: Atp5i	Ion transmembrane transporter activity	ATP synthase E chain

TABLE II—*continued*

IPI number and gene name	Functional relevance[a]	Pfam descriptions
IPI00314709: Sfrs5[c]	RNA binding	RNA recognition motif
IPI00126396: Mcm7	DNA replication initiation	MCM2/3/5 family
IPI00331143: Dnmt3b	DNA (cytosine-5-)-methyltransferase activity	C-5 cytosine-specific DNA methylase
IPI00317740: Gnb2l1		WD domain, G-beta repeat
IPI00170008: Snrpa1	mRNA processing	
IPI00134621: Ran[b,c]	Nucleocytoplasmic transport	Ras family
IPI00130280: Atp5a1	Purine nucleotide biosynthetic process	ATP synthase alpha/beta family
IPI00474430: Sfrs2	RNA splicing	RNA recognition motif
IPI00307837: Eef1a1	Translation factor activity	Elongation factor Tu GTP binding domain

[a] According to Gene Ontology.
[b] Proteins previously shown to associate directly or indirectly with β-catenin according to literature search.
[c] Proteins that were found with ratios of more than 1.5 in the biological replicas in both the Wnt3a-independent and Wnt3a-dependent proteomes.

among the proteins that had ratios of less than 1.5 after Wnt3a stimulation. This suggests that these 64 proteins formed stable complexes with β-catenin that were not affected by Wnt3a treatment. Between the Wnt3a-independent and -dependent interactomes there was an overlap of seven proteins: VDAC1, RAN, SFRS5, HMG2, HNRNPA1, ELAVL1, and RAB1A (supplemental Fig. S2*B*). These proteins represent a subset of binding partners that interact with β-catenin in the chromatin of mES cells, and this interaction is potentiated upon exogenous activation of canonical Wnt signaling.

GO Term Enrichment Analysis—To determine in which processes the identified β-catenin interaction partners are involved, we performed molecular function, biological process, and cellular component GO term enrichment analysis of the β-catenin Wnt3a-independent and -dependent interactomes (supplemental Fig. S3, supplemental Tables S5 and S6). In both interactomes there were gene functions associated with protein binding (GO:000551), nucleic acid binding (GO:0003676), and small molecule binding (GO:0036094) (supplemental Figs. S3*B* and S3*D*), as well as various GO functions associated with metabolism and gene expression (supplemental Figs. S3*A* and S3*C*). Interestingly, however, in the Wnt3a-independent proteome there was overrepresentation of gene functions associated with DNA binding (GO:0003677) and nucleoside binding (GO:0001882), whereas in the Wnt3a-dependent proteome there was enrichment of gene functions associated with RNA binding (GO:0003723), translation factor activity, nucleic acid binding (GO:0008135), and translational elongation factor activity (GO:0003746) (supplemental Figs. S3*B* and S3*D*). Furthermore, in the Wnt3a-independent proteome there were clusters of gene functions associated with chromosome organization (GO:0051276), chromatin remodeling complex (GO:0016585), and chromatin organization (GO:0006325), whereas in the Wnt3a-dependent proteome there was enrichment in gene functions associated with RNA processing (GO:0006396), nuclear export (GO:0051168), transport (GO:0006810), and nucleocytoplasmic transport (GO:0006913) (supplemental Figs. S3*A* and S3*C*). These findings imply overlapping, but also functions of β-catenin in mES cells with or without Wnt3a stimulation.

Screen Validation—To assess the quality of the screen, we decided to test some of the identified proteins from both the Wnt3a-dependent and the Wnt3a-independent β-catenin interactomes that had not been previously characterized for their ability to bind β-catenin in different biochemical and cellular assays. We used specific anti-β-catenin antibodies to immunoprecipitate the endogenous β-catenin from W4 wild-type mES, and we used Western blot to test for the co-purification of SALL4 and LSD1, two proteins that were found in the Wnt3a-independent β-catenin interactome. SALL4 is a transcription factor essential for the self-renewal of mES cells, and it exerts its function by directly binding two other key transcription factors in mES cells, Nanog and Oct4 (26–30). LSD1 is a histone demethylase that participates both in silencing complexes by catalyzing the demethylation of both di- and monomethylated lysine 4 (H3K4me2/1) and in activating complexes, where it demethylates lysine 9 of histone H3 (H3K9me2/1) (31, 32). mES cells deficient for LSD1 show a precautious expression of developmental markers and a loss in global levels of DNA methylation (33, 34).

We could specifically co-immunoprecipitate SALL4 with anti-β-catenin antibody (Fig. 4*A*, upper panel). Reciprocally, β-catenin could be specifically co-immunoprecipitated with an anti-SALL4 antibody (Fig. 4*A*, lower panel). Similarly, we were able to co-immunoprecipitate LSD1 from W4 cells using an anti-β-catenin antibody (Fig 4*B*, upper panel), and vice versa, we were able to co-immunoprecipitate β-catenin using an anti-LSD1 antibody (Fig. 4*B*, lower panel). These results support our SILAC-MS screen.

To confirm that the LSD1/β-catenin and SALL4/β-catenin interactions indeed take place within the chromatin of wild-type mES cells, we used a cell-based proximity ligation assay (35, 36). This method is suitable for visualizing protein interactions *in situ* and provides information about the localization of protein complexes. It relies on the use of protein-specific primary antibodies and secondary antibodies with attached

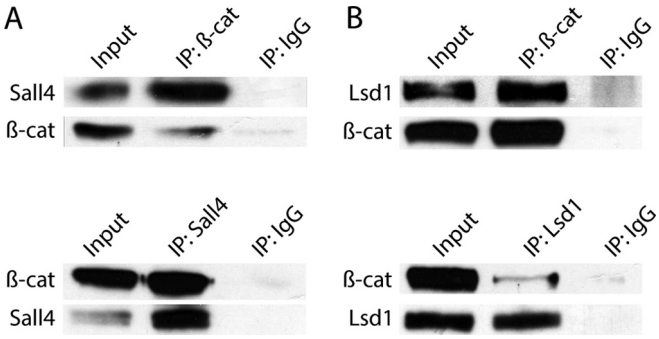

FIG. 4. **LSD1 and SALL4 can be co-purified with endogenous β-catenin from the chromatin of wild-type mES cells.** *A*, co-immunoprecipitations of endogenous SALL4 and β-catenin from chromatin of W4 cells with anti-β-catenin and anti-SALL4 antibodies. *B*, co-immunoprecipitations from nuclear extracts of W4 cells of endogenous LSD1 and β-catenin with anti-β-catenin and anti-LSD1 antibodies.

DNA strands that participate in ligation, replication, and sequence decoding reactions (35, 37). As a control, we used 16.1 cells, which are β-catenin deficient (38). By using specific anti-β-catenin and anti-SALL4 antibodies, we detected the SALL4/β-catenin interaction in the chromatin of wild-type W4 mES cells, but not in the chromatin of control 16.1 mES cells (Fig. 5*A*). Similarly, we were able to detect the interaction of β-catenin and LSD1 in the nuclei of wild-type W4 mES cells, but not in the nuclei of control 16.1 mES cells (Fig. 5*B*). Thus, these results validated the correct subcellular localization of the novel β-catenin complexes that we uncovered with our SILAC-based screen.

From the Wnt3a-dependent interactome, we set out to validate the interaction of β-catenin with Hmg2. This protein has already been shown to form functional complexes with β-catenin in the superficial zone of articular cartilage that are essential for the maintenance of tissue homeostasis (39). This interaction is indirect via Lef-1 and is controlled by the canonical Wnt signaling (39). Interestingly, however, in our mES cell model, β-catenin was found to bind Hmg2 in the Wnt3a-independent interactome, but the complex formation was further enhanced by the addition of exogenous Wnt3a (Tables I and II). We used the proximity ligation assay with anti-β-catenin and anti-Hmg2 antibodies and compared the complex formation in W4 wild-type mES cells that were either treated with Wnt3a for 4 h or mock-treated. We found that the β-catenin–Hmg2 complexes were readily observed in mock-treated W4 cells, but the signal was increased after treatment with Wnt3a (Fig. 5*C*). Hmg2 is a nonspecific DNA-binding and -bending protein that facilitates the formation of complex nucleoprotein complexes involved in the regulation of gene expression (40–43). Therefore, it is possible that the enhancement of the β-catenin–Hmg2 interaction upon Wnt3a treatment reflects the active β-catenin-dependent restructuring of the chromatin.

Functional Characterization of the β-catenin–LSD1 Interaction—To validate the functional relevance of our screen, we decided to study the significance of the β-catenin–LSD1 interaction in the regulation of gene expression. It was recently shown that LSD1 binds to a proximal enhancer of *Lefty1* and regulates *Lefty1* expression in mES cells by controlling the methylation status of H3K4 (14, 44). *Lefty1* encodes a transforming growth factor beta (TGFβ) superfamily protein (45) that antagonizes the functions of *Activin* and *Nodal* and is essential in the establishment of left-right asymmetry of the embryo (46, 47). It has been suggested that the function of *Lefty1* in stem cells is to protect them from the action of developmental inducers (48). We found that *Lefty1* is one of the early genes that become up-regulated in SR1-Cre-ERT2 mES cells after the addition of tamoxifen (Fig. 6*D*). This suggests that *Lefty1* is a direct target of β-catenin and that β-catenin participates in a repressive complex that controls *Lefty1* expression, possibly with LSD1. We hypothesized that β-catenin and LSD1 are recruited to the very same enhancer. To test this hypothesis, we carried out chromatin immunoprecipitations with anti-LSD1 and anti-β-catenin antibodies in SR1-Cre-ERT2 cells mock-treated or treated with tamoxifen, and we amplified the genomic sequences corresponding to the previously characterized enhancer of *Lefty1* (14). Interestingly, we found that both β-catenin and LSD1 were bound to the *Lefty1* enhancer in SR1-Cre-ERT2 cells, but this binding was greatly diminished upon the removal of functional β-catenin (Figs. 6*A*, 6*B*). This suggests that the formation of the repressive complex on the *Lefty1* enhancer is dependent on the presence of functional β-catenin. To show that the formation of the β-catenin–LSD1 complex is functionally relevant, we tested the levels of H3K4me2/3 at the *Lefty1* enhancer. We found that the H3K4me2/3 levels at the *Lefty1* enhancer, which mark active genes, increased upon the removal of functional β-catenin (Fig. 6*C*). Our findings suggest that a repressive complex containing β-catenin and LSD1 controls the levels of *Lefty1* in mES cells. The recruitment of LSD1 to the *Lefty1* enhancer, and thereby the demethylation of H3K4me2/3, is dependent on the presence of β-catenin at this enhancer.

β-catenin and LSD1 Expression Levels Are Inversely Correlated with Lefty1 Expression Levels in Pancreas Cancer Cells and in the Normal Epithelium of Breast Cancer Patients—*Lefty1* has been recently identified as a tumor suppressor in human pancreas cancer cells (49). We used publically available data (PubMed ID 19260470) to compare the mRNA expression levels of *β-catenin* and *LSD1* with those of *Lefty1* in pancreas cancer tumors (50). Interestingly, the mRNA expression levels of *β-catenin* and *LSD1* were inversely correlated with those of *Lefty1* ($r = -0.39$ and $r = -0.49$, respectively), which is in agreement with our data from the mES cell model (Figs. 7*A*, 7*C*). Importantly, this correlation is not unique to pancreas cancer and can be observed in pre-malignant tissues. We compared the mRNA expression levels of *β-catenin* and *LSD1* with those of *Lefty1* first in histologically normal breast epithelium of non-cancer controls, and second in the

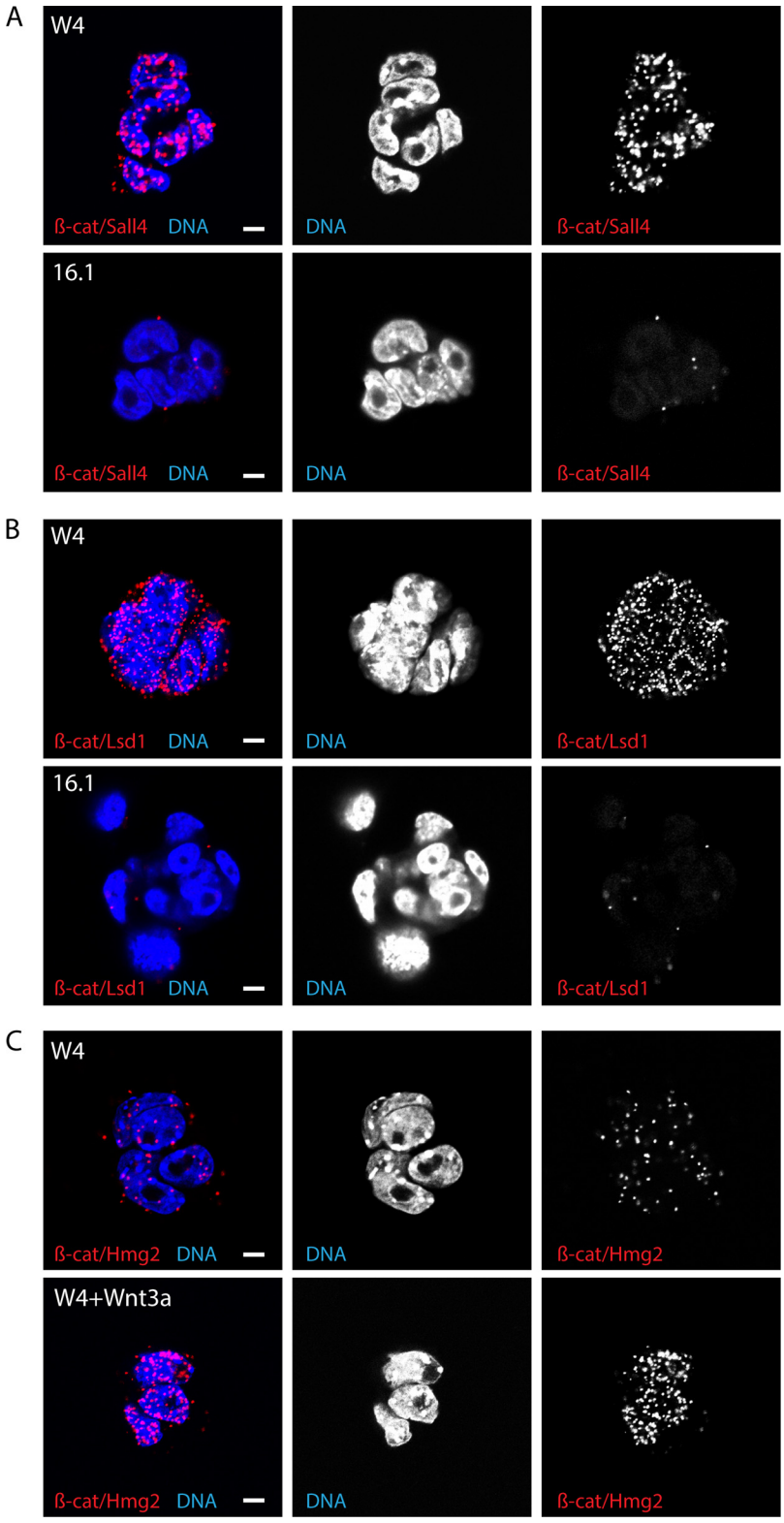

FIG. 5. **Biochemically identified β-catenin-associated proteins interact with β-catenin *in vivo*.** *A*, proximity ligation assay (PLA) of SALL4/β-catenin in wild-type (W4) cells and β-catenin$^{-/-}$ (16. 1) cells. *B*, PLA of LSD1/β-catenin in W4 and 16.1 cells. *C*, PLA of HMG2/β-catenin in W4 cells without and with Wnt3a stimulation. DNA was stained with DAPI. In each panel, the individual channels of the confocal image are shown next to the merged image. Scale bars correspond to 5 μm.

histologically normal breast epithelium of breast cancer patients (PubMed ID 20197764) (51). In the non-cancer controls we found no correlation between the expression levels of *β-catenin* and *Lefty1* ($r = -0.15$; supplemental Fig. S4*A*) or between the expression levels of *LSD1* and *Lefty1* ($r = -0.04$; supplemental Fig. S4*B*). Interestingly, in the normal epithelium of breast cancer patients there was a negative correlation between the expression levels of *β-catenin* and those of

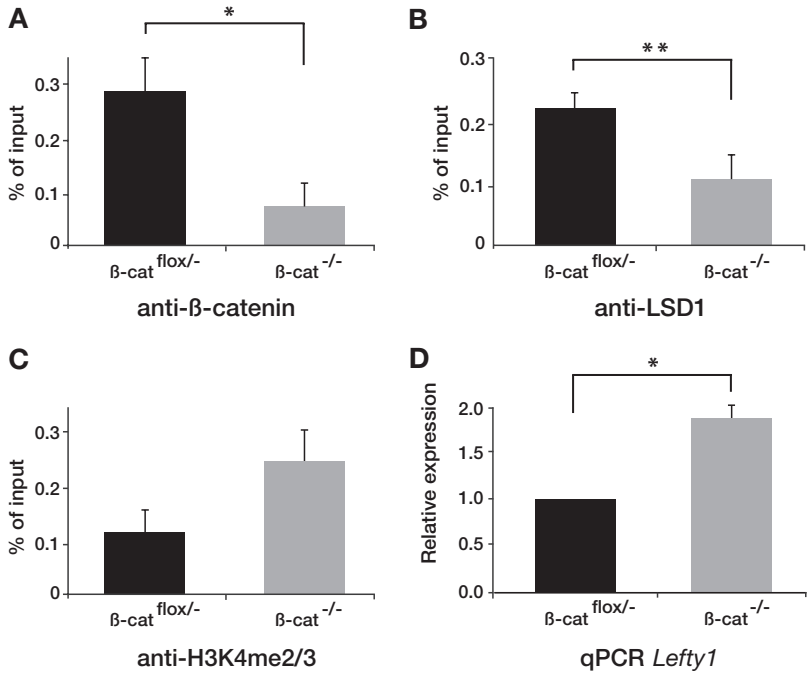

FIG. 6. **β-catenin and LSD1 regulate the expression of *Lefty1* by controlling the levels of H3K4me2/3 at the *Lefty1* proximal enhancer.** Chromatin immunoprecipitations with (*A*) anti-β-catenin, (*B*) anti-LSD1, and (*C*) anti-H3K4me2/3 antibodies of the *Lefty1* enhancer before (*β-cat$^{flox/-}$*) and 3 days after (*β-cat$^{-/-}$*) treatment with (Z)-4-hydroxytamoxifen. The noise (IgG control) was subtracted from the signal before plotting. *D*, qPCR for *Lefty1* in SR1-Cre-ERT2 before (*β-cat$^{flox/-}$*) and 3 days after (*β-cat$^{-/-}$*) treatment with (Z)-4-hydroxytamoxifen. In all experiments, the statistically significant differences are represented with asterisks; * stands for $p < 0.05$, and ** stands for $p < 0.01$.

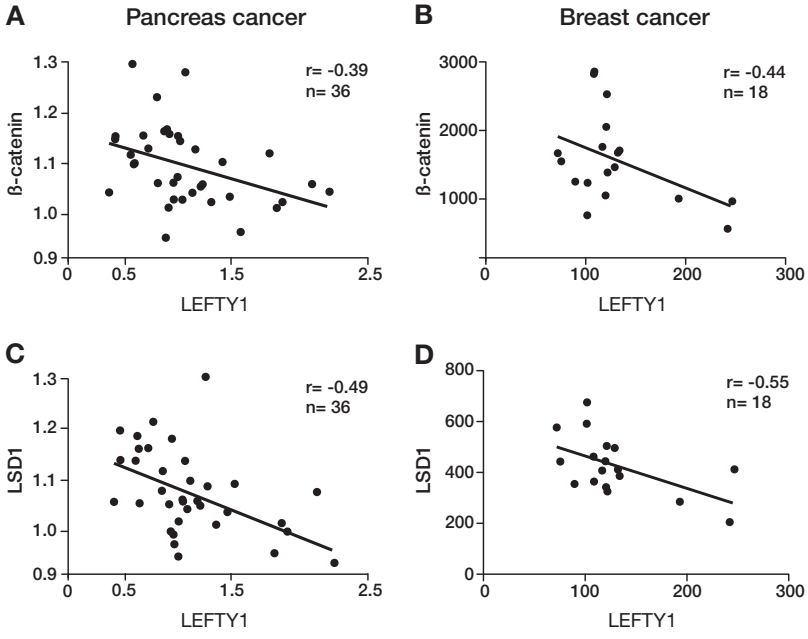

FIG. 7. ***Lefty1* mRNA expression levels are inversely correlated with the expression levels of *β-catenin* and *LSD1* in the pancreas cancer and in the normal epithelium of breast cancer patients.** Correlation analysis between the mRNA expression levels of *Lefty1* and β-catenin (*A*, *B*) and *Lefty1* and LSD1 (*C*, *D*) in pancreas cancer tissue *versus* non-cancer tissue from the same patient (*A*, *C*) and in the normal epithelium of breast cancer patients (*B*, *D*). *r*, Pearson correlation coefficient; *n*, number of samples.

Lefty1 ($r = -0.44$), as well as between the expression levels of *LSD1* and those of *Lefty1* ($r = -0.55$) (Figs. 7*B*, 7*D*). Taken together with our data, this implies that the down-regulation of the tumor suppressor *Lefty1* by β-catenin and LSD1 might be an early event in malignant transformation.

DISCUSSION

We used affinity purifications and SILAC-MS to study the interactome of chromatin-bound β-catenin in mES cells under standard culturing conditions and after treatment with Wnt3a. We identified 76 proteins from the Wnt3a-independent interactome and 69 proteins from the Wnt3a-dependent interactome of β-catenin. We showed that β-catenin uses the demethylase activity of one of its newly identified interaction partners, LSD1, to regulate the expression of *Lefty1* in mES cells. Both LSD1 and β-catenin bind to the proximal enhancer of *Lefty1*, and the recruitment of LSD1 to the *Lefty1* enhancer and the H3K4me2/3 levels at this enhancer are dependent on β-catenin. *LSD1* and *β-catenin* mRNA levels are inversely correlated with the levels of *Lefty1* in human tumors.

Our work identified an extensive network of protein interactions of β-catenin in mES cells. 80% of the newly identified

proteins in the Wnt3a-independent proteome and 90% of those in the Wnt3a-dependent proteome are novel interaction partners. Interestingly, most of the proteins that were identified in the Wnt3a-independent interactome of β-catenin showed a normalized ratio of less than 1.5 in the Wnt3a-dependent interactome. This implies that these interactions are rather stable and are not influenced by additional Wnt3a stimulation. Seven proteins of the Wnt3a-independent interactome were also specifically enriched in the Wnt3a-dependent interactome. Their interaction with β-catenin appeared to get stronger with increasing levels of β-catenin. One explanation for that would be that these proteins participate in the formation of new β-catenin complexes. For example, Hmg2 is a nonspecific DNA-binding and DNA-bending protein (43), and the interaction with β-catenin could be one of the early events in the formation of β-catenin-containing complexes.

Recently, it has been shown that β-catenin can be recruited to target genes in mES cells not only by the canonical Tcf transcription factors (52), but also by OCT-3/4 (53, 54) and KLF4 (38). Interestingly, we found that in the Wnt3a-independent interactome, β-catenin associates with SALL4, another transcription factor that is part of the core pluripotency network (27, 28, 30). One implication of that fact would be that some yet-to-be-identified genes might be regulated through the β-catenin–SALL4 interaction and, probably, through associated chromatin-modifying activity. One candidate for such activity would be the Mi2–nucleosome remodeling and deacetylase (NuRD) complex. SALL4 was shown to repress the expression of the stem cell factors SALL1 and PTEN through the recruitment of the Mi2–NuRD complex in human embryonic stem cells (55). The Mi2–NuRD complex utilizes the histone deacetylase activity of Hdac1 or Hdac2 to silence its targets, which in mES cells include the pluripotency genes *Zfp42*, *Tbx3*, *Klf4*, and *Klf5* (55). Indeed, we found two components of the Mi2/NuRD complex in our screen: Hdac1 and Gatad2a (56). Gatad2a (p66) has already been genetically identified as a component of canonical Wnt signaling in the fly (57), implicating the Mi2–NuRD complex in the repression of Wnt target genes. Our studies suggest that in mES cells, Wnt signaling and the Mi2–NuRD complex meet at the level of β-catenin. Further studies are required in order to test whether SALL4–Mi2–NuRD–β-catenin complexes can form on target promoters. To identify putative target genes, it would be essential to compare the genome-wide binding sites of SALL4 in mES cells with those of β-catenin and of Mi2–NuRD.

Besides its histone deacetylase activity, the Mi2–NuRD complex has been shown recently to associate with the H3K4me2/1 demethylase LSD1 in cancer cells (58). In embryonic stem cells, LSD1 co-occupies nine of every ten enhancers with the NuRD complex, suggesting a significant functional overlap (14). Interestingly, we identified LSD1 as a novel interaction partner of β-catenin in the Wnt3a-independent interactome. In human breast cancer cells, the Mi2–NuRD–LSD1 complex suppresses the expression of members of the TGFβ1 signaling pathway (58). At least one member of the TGFβ signaling pathway, *Lefty1*, has been shown to be a direct transcriptional target of LSD1 in embryonic stem cells (14). *Lefty1* is a nodal antagonist that has recently been shown to act as a tumor suppressor in pancreatic cancer (49). We found that *Lefty1* is up-regulated in β-catenin$^{-/-}$ mES cells and that β-catenin is recruited to the proximal enhancer of *Lefty1*. The active enhancers in embryonic stem cells, including the *Lefty1* enhancer, are marked by H3K4me1 and H3K4me2, but not by H3K4me3 (14, 59, 60). By using an anti-H3K4me2/3 antibody, we showed that the demethylase activity of LSD1 at the *Lefty1* enhancer is dependent on β-catenin, implying that β-catenin recruits LSD1 to the *Lefty1* enhancer. Recently, it was also found that SALL4 binds the proximal enhancer of *Lefty1* (14). It is tempting to speculate that, at this particular enhancer, a tertiary complex of SALL4–β-catenin–LSD1 might form. The regulation of *Lefty1* expression by LSD1 and β-catenin might not be restricted to the mES cell model. Indeed, we found that the levels of *Lefty1* are inversely correlated with those of β-catenin and LSD1 in pancreatic cancer and in pre-malignant breast cancer epithelium. Thus, the mechanism of repression of the tumor suppressor *Lefty1* by β-catenin and LSD1 might be common to mES cells and cancer cells, and this mechanism could provide novel therapeutic targets for human disease.

Acknowledgments—We thank Dr. Gerhard Mittler from the Proteomics Facility of the Max Planck Institute of Immunobiology and Epigenetics, Freiburg, Germany, for the kindly provided mass spectroscopy service.

S This article contains supplemental material.

¶ To whom correspondence should be addressed: Tel.: +49 761 5108 471, Fax: +49 761 5108 474. E-mail: kemler@ie-freiburg.mpg.de.

REFERENCES

1. Clevers, H. (2006) Wnt/β-catenin signaling in development and disease. *Cell* **127,** 469–480
2. Mosimann, C., Hausmann, G., and Basler, K. (2009) β-Catenin hits chromatin: regulation of Wnt target gene activation. *Nat. Rev. Mol. Cell Biol.* **10,** 276–286
3. Roeder, R. G. (2005) Transcriptional regulation and the role of diverse coactivators in animal cells. *FEBS Lett.* **579,** 909–915
4. Li, M., Liu, G.-H., and Belmonte, J. C. I. (2012) Navigating the epigenetic landscape of pluripotent stem cells. *Nat. Rev. Mol. Cell Biol.* **13,** 524–535
5. Bernstein, B. E., Mikkelsen, T. S., Xie, X., Kamal, M., Huebert, D. J., Cuff, J., Fry, B., Meissner, A., Wernig, M., Plath, K., Jaenisch, R., Wagschal, A., Feil, R., Schreiber, S. L., and Lander, E. S. (2006) A bivalent chromatin structure marks key developmental genes in embryonic stem cells. *Cell* **125,** 315–326
6. Sokol, S. Y. (2011) Maintaining embryonic stem cell pluripotency with Wnt signaling. *Development* **138,** 4341–4350
7. Ogawa, K., Nishinakamura, R., Iwamatsu, Y., Shimosato, D., and Niwa, H. (2006) Synergistic action of Wnt and LIF in maintaining pluripotency of mouse ES cells. *Biochem. Biophys. Res. Commun.* **343,** 159–166
8. Blagoev, B., Ong, S.-E., Kratchmarova, I., and Mann, M. (2004) Temporal analysis of phosphotyrosine-dependent signaling networks by quantitative proteomics. *Nat. Biotechnol.* **22,** 1139–1145
9. Shevchenko, A., Tomas, H., Havlis, J., Olsen, J. V., and Mann, M. (2007) In-gel digestion for mass spectrometric characterization of proteins and

proteomes. *Nat. Protoc.* **1,** 2856–2860
10. Cox, J., and Mann, M. (2008) MaxQuant enables high peptide identification rates, individualized p.p.b.-range mass accuracies and proteome-wide protein quantification. *Nat. Biotechnol.* **26,** 1367–1372
11. Carbon, S., Ireland, A., Mungall, C. J., Shu, S., Marshall, B., and Lewis, S. (2009) AmiGO: online access to ontology and annotation data. *Bioinformatics* **25,** 288–289
12. Supek, F., Bošnjak, M., Škunca, N., and Šmuc, T. (2011) REVIGO summarizes and visualizes long lists of Gene Ontology terms. *PLoS One* **6,** e21800
13. Development Core Team (2005) *R: A Language and Environment for Statistical Computing*, R Foundation for Statistical Computing, Vienna, Austria
14. Whyte, W. A., Bilodeau, S., Orlando, D. A., Hoke, H. A., Frampton, G. M., Foster, C. T., Cowley, S. M., and Young, R. A. (2012) Enhancer decommissioning by LSD1 during embryonic stem cell differentiation. *Nature* **482,** 221–225
15. Szklarczyk, D., Franceschini, A., Kuhn, M., Simonovic, M., Roth, A., Minguez, P., Doerks, T., Stark, M., Muller, J., Bork, P., Jensen, L. J., and Von Mering, C. (2011) The STRING database in 2011: functional interaction networks of proteins, globally integrated and scored. *Nucleic Acids Res.* **39,** D561–D568
16. Brault, V., Moore, R., Kutsch, S., Ishibashi, M., Rowitch, D. H., McMahon, A. P., Sommer, L., Boussadia, O., and Kemler, R. (2001) Inactivation of the (β)-catenin gene by Wnt1-Cre-mediated deletion results in dramatic brain malformation and failure of craniofacial development. *Development* **128,** 1253–1264
17. Feil, R., Wagner, J., Metzger, D., and Chambon, P. (1997) Regulation of Cre recombinase activity by mutated estrogen receptor ligand-binding domains. *Biochem. Biophys. Res. Commun.* **237,** 752–757
18. Ozawa, M., Baribault, H., and Kemler, R. (1989) The cytoplasmic domain of the cell adhesion molecule uvomorulin associates with three independent proteins structurally related in different species. *EMBO J.* **8,** 1711–1717
19. Boyer, L. A., Lee, T. I., Cole, M. F., Johnstone, S. E., Levine, S. S., Zucker, J. P., Guenther, M. G., Kumar, R. M., Murray, H. L., Jenner, R. G., Gifford, D. K., Melton, D. A., Jaenisch, R., and Young, R. A. (2005) Core transcriptional regulatory circuitry in human embryonic stem cells. *Cell* **122,** 947–956
20. Nichols, J., Zevnik, B., Anastassiadis, K., Niwa, H., Klewe-Nebenius, D., Chambers, I., Schöler, H., and Smith, A. (1998) Formation of pluripotent stem cells in the mammalian embryo depends on the POU transcription factor Oct4. *Cell* **95,** 379–391
21. Hay, D. C., Sutherland, L., Clark, J., and Burdon, T. (2004) Oct-4 knockdown induces similar patterns of endoderm and trophoblast differentiation markers in human and mouse embryonic stem cells. *Stem Cells* **22,** 225–235
22. Shelton, K. R., Egle, P. M., and Cochran, D. L. (1981) Nuclear envelope proteins: identification of lamin B subtypes. *Biochem. Biophys. Res. Commun.* **103,** 975–981
23. Bauer, A., Huber, O., and Kemler, R. (1998) Pontin52, an interaction partner of β-catenin, binds to the TATA box binding protein. *Proc. Natl. Acad. Sci. U.S.A.* **95,** 14787–14792
24. Bauer, A., Chauvet, S., Huber, O., Usseglio, F., Rothbächer, U., Aragnol, D., Kemler, R., and Pradel, J. (2000) Pontin52 and Reptin52 function as antagonistic regulators of β-catenin signalling activity. *EMBO J.* **19,** 6121–6130
25. Rudloff, S., and Kemler, R. (2012) Differential requirements for β-catenin during mouse development. *Development* **139,** 3711–3721
26. Wang, J., Rao, S., Chu, J., Shen, X., Levasseur, D. N., Theunissen, T. W., and Orkin, S. H. (2006) A protein interaction network for pluripotency of embryonic stem cells. *Nature* **444,** 364–368
27. Elling, U., Klasen, C., Eisenberger, T., Anlag, K., and Treier, M. (2006) Murine inner cell mass-derived lineages depend on Sall4 function. *Proc. Natl. Acad. Sci. U.S.A.* **103,** 16319–16324
28. Wu, Q., Chen, X., Zhang, J., Loh, Y.-H., Low, T.-Y., Zhang, W., Zhang, W., Sze, S.-K., Lim, B., and Ng, H.-H. (2006) Sall4 interacts with Nanog and co-occupies Nanog genomic sites in embryonic stem cells. *J. Biol. Chem.* **281,** 24090–24094
29. Sakaki-Yumoto, M., Kobayashi, C., Sato, A., Fujimura, S., Matsumoto, Y., Takasato, M., Kodama, T., Aburatani, H., Asashima, M., Yoshida, N., and Nishinakamura, R. (2006) The murine homolog of SALL4, a causative gene in Okihiro syndrome, is essential for embryonic stem cell proliferation, and cooperates with Sall1 in anorectal, heart, brain and kidney development. *Development* **133,** 3005–3013
30. Zhang, J., Tam, W.-L., Tong, G. Q., Wu, Q., Chan, H.-Y., Soh, B.-S., Lou, Y., Yang, J., Ma, Y., Chai, L., Ng, H.-H., Lufkin, T., Robson, P., and Lim, B. (2006) Sall4 modulates embryonic stem cell pluripotency and early embryonic development by the transcriptional regulation of Pou5f1. *Nat. Cell Biol.* **8,** 1114–1123
31. Shi, Y., Lan, F., Matson, C., Mulligan, P., Whetstine, J. R., Cole, P. A., Casero, R. A., and Shi, Y. (2004) Histone demethylation mediated by the nuclear amine oxidase homolog LSD1. *Cell* **119,** 941–953
32. Metzger, E., Wissmann, M., Yin, N., Müller, J. M., Schneider, R., Peters, A. H. F. M., Günther, T., Buettner, R., and Schüle, R. (2005) LSD1 demethylates repressive histone marks to promote androgen-receptor-dependent transcription. *Nature* **437,** 436–439
33. Wang, J., Hevi, S., Kurash, J. K., Lei, H., Gay, F., Bajko, J., Su, H., Sun, W., Chang, H., Xu, G., Gaudet, F., Li, E., and Chen, T. (2008) The lysine demethylase LSD1 (KDM1) is required for maintenance of global DNA methylation. *Nat. Genet.* **41,** 125–129
34. Foster, C. T., Dovey, O. M., Lezina, L., Luo, J. L., Gant, T. W., Barlev, N., Bradley, A., and Cowley, S. M. (2010) Lysine-specific demethylase 1 regulates the embryonic transcriptome and CoREST stability. *Mol. Cell. Biol.* **30,** 4851–4863
35. Fredriksson, S., Gullberg, M., Jarvius, J., Olsson, C., Pietras, K., Gústafsdóttir, S. M., Östman, A., and Landegren, U. (2002) Protein detection using proximity-dependent DNA ligation assays. *Nat. Biotechnol.* **20,** 473–477
36. Söderberg, O., Leuchowius, K.-J., Gullberg, M., Jarvius, M., Weibrecht, I., Larsson, L.-G., and Landegren, U. (2008) Characterizing proteins and their interactions in cells and tissues using the in situ proximity ligation assay. *Methods* **45,** 227–232
37. Gullberg, M., Gústafsdóttir, S. M., Schallmeiner, E., Jarvius, J., Bjarnegård, M., Betsholtz, C., Landegren, U., and Fredriksson, S. (2004) Cytokine detection by antibody-based proximity ligation. *Proc. Natl. Acad. Sci. U.S.A.* **101,** 8420–8424
38. Hoffmeyer, K., Raggioli, A., Rudloff, S., Anton, R., Hierholzer, A., Valle, I. D., Hein, K., Vogt, R., and Kemler, R. (2012) Wnt/β-catenin signaling regulates telomerase in stem cells and cancer cells. *Science* **336,** 1549–1554
39. Taniguchi, N., Caramés, B., Kawakami, Y., Amendt, B. A., Komiya, S., and Lotz, M. (2009) Chromatin protein HMGB2 regulates articular cartilage surface maintenance via β-catenin pathway. *Proc. Natl. Acad. Sci. U.S.A.* **106,** 16817–16822
40. Lorenz, M., Hillisch, A., Payet, D., Buttinelli, M., Travers, A., and Diekmann, S. (1999) DNA bending induced by high mobility group proteins studied by fluorescence resonance energy transfer. *Biochemistry* **38,** 12150–12158
41. Boonyaratanakornkit, V., Melvin, V., Prendergast, P., Altmann, M., Ronfani, L., Bianchi, M. E., Taraseviciene, L., Nordeen, S. K., Allegretto, E. A., and Edwards, D. P. (1998) High-mobility group chromatin proteins 1 and 2 functionally interact with steroid hormone receptors to enhance their DNA binding in vitro and transcriptional activity in mammalian cells. *Mol. Cell. Biol.* **18,** 4471–4487
42. Stros, M., Ozaki, T., Bacikova, A., Kageyama, H., and Nakagawara, A. (2002) HMGB1 and HMGB2 cell-specifically down-regulate the p53- and p73-dependent sequence-specific transactivation from the human Bax gene promoter. *J. Biol. Chem.* **277,** 7157–7164
43. Paull, T. T., Haykinson, M. J., and Johnson, R. C. (1993) The nonspecific DNA-binding and -bending proteins HMG1 and HMG2 promote the assembly of complex nucleoprotein structures. *Genes Dev.* **7,** 1521–1534
44. Nakatake, Y., Fukui, N., Iwamatsu, Y., Masui, S., Takahashi, K., Yagi, R., Yagi, K., Miyazaki, J., Matoba, R., Ko, M. S. H., and Niwa, H. (2006) Klf4 cooperates with Oct3/4 and Sox2 to activate the Lefty1 core promoter in embryonic stem cells. *Mol. Cell. Biol.* **26,** 7772–7782
45. Saijoh, Y., Fujii, H., Meno, C., Sato, M., Hirota, Y., Nagamatsu, S., Ikeda, M., and Hamada, H. (1996) Identification of putative downstream genes of Oct-3, a pluripotent cell-specific transcription factor. *Genes Cells* **1,** 239–252
46. Meno, C., Gritsman, K., Ohishi, S., Ohfuji, Y., Heckscher, E., Mochida, K., Shimono, A., Kondoh, H., Talbot, W. S., Robertson, E. J., Schier, A. F.,

and Hamada, H. (1999) Mouse Lefty2 and zebrafish Antivin are feedback inhibitors of nodal signaling during vertebrate gastrulation. *Mol. Cell* **4,** 287–298
47. Meno, C., Shimono, A., Saijoh, Y., Yashiro, K., Mochida, K., Ohishi, S., Noji, S., Kondoh, H., and Hamada, H. (1998) Lefty-1 is required for left-right determination as a regulator of lefty-2 and nodal. *Cell* **94,** 287–297
48. Niwa, H., Masui, S., Chambers, I., Smith, A. G., and Miyazaki, J. (2002) Phenotypic complementation establishes requirements for specific POU domain and generic transactivation function of Oct-3/4 in embryonic stem cells. *Mol. Cell. Biol.* **22,** 1526–1536
49. Miyata, N., Azuma, T., Hozawa, S., Higuchi, H., Yokoyama, A., Kabashima, A., Igarashi, T., Saeki, K., and Hibi, T. (2012) Transforming growth factor β and Ras/MEK/ERK signaling regulate the expression level of a novel tumor suppressor Lefty. *Pancreas* **41,** 745–752
50. Badea, L., Herlea, V., Dima, S. O., Dumitrascu, T., and Popescu, I. (2008) Combined gene expression analysis of whole-tissue and microdissected pancreatic ductal adenocarcinoma identifies genes specifically overexpressed in tumor epithelia. *Hepatogastroenterology* **55,** 2016–2027
51. Graham, K., de las Morenas, A., Tripathi, A., King, C., Kavanah, M., Mendez, J., Stone, M., Slama, J., Miller, M., Antoine, G., Willers, H., Sebastiani, P., and Rosenberg, C. L. (2010) Gene expression in histologically normal epithelium from breast cancer patients and from cancer-free prophylactic mastectomy patients shares a similar profile. *Br. J. Cancer* **102,** 1284–1293
52. Yi, F., Pereira, L., Hoffman, J. A., Shy, B. R., Yuen, C. M., Liu, D. R., and Merrill, B. J. (2011) Opposing effects of Tcf3 and Tcf1 control Wnt stimulation of embryonic stem cell self-renewal. *Nat. Cell Biol.* **13,** 762–770
53. Kelly, K. F., Ng, D. Y., Jayakumaran, G., Wood, G. A., Koide, H., and Doble, B. W. (2011) β-catenin enhances Oct-4 activity and reinforces pluripotency through a TCF-independent mechanism. *Cell Stem Cell* **8,** 214–227
54. Abu-Remaileh, M., Gerson, A., Farago, M., Nathan, G., Alkalay, I., Rousso, S. Z., Gur, M., Fainsod, A., and Bergman, Y. (2010) Oct-3/4 regulates stem cell identity and cell fate decisions by modulating Wnt/β-catenin signalling. *EMBO J.* **29,** 3236–3248
55. Lu, J., Jeong, H., Kong, N., Yang, Y., Carroll, J., Luo, H. R., Silberstein, L. E., Yupo, M., and Chai, L. (2009) Stem cell factor SALL4 represses the transcriptions of PTEN and SALL1 through an epigenetic repressor complex. *PLoS One* **4,** e5577
56. Denslow, S. A., and Wade, P. A. (2007) The human Mi-2/NuRD complex and gene regulation. *Oncogene* **26,** 5433–5438
57. Kon, C., Cadigan, K. M., Da Silva, S. L., and Nusse, R. (2005) Developmental roles of the Mi-2/NURD-associated protein p66 in Drosophila. *Genetics* **169,** 2087–2100
58. Wang, Y., Zhang, H., Chen, Y., Sun, Y., Yang, F., Yu, W., Liang, J., Sun, L., Yang, X., Shi, L., Li, R., Li, Y., Zhang, Y., Li, Q., Yi, X., and Shang, Y. (2009) LSD1 is a subunit of the NuRD complex and targets the metastasis programs in breast cancer. *Cell* **138,** 660–672
59. Heintzman, N. D., Stuart, R. K., Hon, G., Fu, Y., Ching, C. W., Hawkins, R. D., Barrera, L. O., Van Calcar, S., Qu, C., Ching, K. A., Wang, W., Weng, Z., Green, R. D., Crawford, G. E., and Ren, B. (2007) Distinct and predictive chromatin signatures of transcriptional promoters and enhancers in the human genome. *Nat. Genet.* **39,** 311–318
60. Lupien, M., Eeckhoute, J., Meyer, C. A., Wang, Q., Zhang, Y., Li, W., Carroll, J. S., Liu, X. S., and Brown, M. (2008) FoxA1 translates epigenetic signatures into enhancer-driven lineage-specific transcription. *Cell* **132,** 958–970